

Published in final edited form as:

Lab Chip. 2011 February 21; 11(4): 599–604. doi:10.1039/c0lc00532k.

Dielectrophoresis of *Caenorhabditis elegans*

Han-Sheng Chuang^a, David Raizen^b, Annesia Lamb^b, Nooreen Dabbish^b, and Haim Bau^{*,a}

^aMechanical Engineering and Applied Mechanics, University of Pennsylvania, Philadelphia, PA, USA

^bDepartment of Neurology, University of Pennsylvania, Philadelphia, PA, USA

Abstract

We demonstrate for the first time the dielectrophoretic trapping and manipulation of a whole animal, the nematode *Caenorhabditis elegans*. We studied the effect of the electric field on the nematode as a function of field intensity and frequency. We identified a range of electric field intensities and frequencies that trap worms without apparent adverse effect on their viability. Worms tethered by dielectrophoresis (DEP) exhibit behavioral responses to blue light, indicating that at least some of the nervous system functions are unimpaired by the electrical field. DEP is useful to dynamically tether nematodes, sort nematodes according to size, and separate dead worms from live ones.

Dielectrophoresis (DEP) has been widely used to trap, position, and sort nano and micro particles, macromolecules, bacteria, and cells¹⁻³. To the best of our knowledge, dielectrophoretic trapping of whole animals has not been previously reported. The dielectrophoretic trapping of animals presents special challenges such as the need to induce sufficiently large electrostatic forces to overcome the animal's muscular force without causing harm. In this communication, we demonstrate that dielectrophoretic forces can be used to trap and manipulate the wild-type *Caenorhabditis elegans* (*C. elegans*).

C. elegans is an attractive animal model for biological and medical research⁴⁻⁹ because of its relatively small size (adult worms are approximately 1 mm long), well-mapped neuronal system, transparency, and relatively short life cycle of 2.5 days. In many studies, it is necessary to select and sort worms and immobilize them for observations¹⁰⁻¹⁴. Current techniques consist of manually picking up an individual worm and gluing the worm to a surface¹⁵, or immobilizing worms in microfluidic channels¹⁶, in which the movement of the worms is typically controlled pneumatically. The ability to manipulate worms with non-contact forces would add a useful tool to researchers' arsenal.

It has been known for some time that *C. elegans* crawls or swims towards the negative electrode in a DC electric field¹⁷⁻¹⁹. This phenomenon has been dubbed electrotaxis^{18, 20}. Electrotaxis is mediated by the worm's sensory nervous system and it affects only relatively mature worms (> L2) possibly because younger worms cannot produce sufficient biological force to overcome electrokinetic forces¹⁷. At higher frequencies (1-3000 Hz), worms are localized in a small region probably due to frequent changes in the direction of

© The Royal Society of Chemistry

*Corresponding author. bau@seas.upenn.edu .

†Electronic Supplementary Information (ESI) available: [details of any supplementary information available should be included here]. See DOI: 10.1039/b000000x/

‡Footnotes should appear here. These might include comments relevant to but not central to the matter under discussion, limited experimental and spectral data, and crystallographic data.

electrotaxis.¹⁷ Here, we investigate the effect of relatively high frequency electric fields on worms. In contrast to electrotaxis, the worms are trapped at the location of the maximum electric field intensity and are insensitive to the field's polarity. The phrase "trapping" in this study refers to tethering the worm to the field of view. We reason that the worms are polarized by the electric field and subjected to a net electrostatic force when the field is non-uniform. DEP offers a number of advantages over other immobilization techniques. Electrodes can be patterned using microfabrication techniques to form intricate, high density structures and apply forces remotely without any direct contact. The forces' magnitude can be readily controlled by adjusting the electrical potentials and worms can be trapped and released on demand.

To study the effects of non-uniform, alternating electric fields on worms, we micropatterned a pair of gold electrodes on a glass slide (Fig. 1a). We employed two different electrode patterns: spiked electrodes (Fig. 1a top) and flat electrodes (Fig. 1a, bottom). A polydimethylsiloxane (PDMS) slab with a molded conduit, 300 μm in width and 118 μm in height, was bonded on the top of a glass slide with the electrode pair aligned with the conduit and centered at the midwidth of the conduit (see Supplementary Data for dimensions and fabrication details). Fig. 1a also depicts top views of the electric field lines associated with both electrode configurations. In the case of the spiked electrodes, the maxima of the electric field intensity are at the tips of electrodes. In the case of the flat electrodes, the maxima are along the edges of the electrodes. Thus, in the latter case, the worm can slide along the surfaces of the electrodes without experiencing any change in the DEP force.

Worms were introduced into the conduit at its inlet and propelled gently towards the location of the electrodes using a syringe pump. In the absence of an electric field, the worms passed undisturbed over the electrodes. When an AC potential difference is applied across the electrodes, an elongated object such as an ellipsoid is polarized (Fig. 1b). The polarization forces induce a torque that aligns the object with the electric field lines. When the electric field is not uniform and the effective polarizability of the object exceeds that of the suspending medium, force²¹

$$F_{dep} = \epsilon_l V \text{Re} [K(\omega)] \nabla |E|^2 \quad (1)$$

will act on the object's center of mass towards the location of maximum electric field intensity. In the above, V is the object's volume; ϵ_l is the electrical permittivity of the suspending medium; $K(\omega)$ is the Clausius-Mossotti factor which accounts for the difference between the object's apparent and the suspending medium's dielectric properties and the object's geometry; and E is the electric field.

We model live and dead worms as multi-shell ellipsoids with and without a membrane, respectively (Fig. 1c). Fig. 1d depicts the estimated Clausius-Mossotti factors of a live worm (blue dashed line) and a dead worm (red solid line) as functions of the electric field frequency (the dielectric properties used in the calculations are available in Table S1 in Supplementary Data). In our model, the live worm has a biological membrane between the cuticle and internal milieu of the worm, which filters low frequency electric fields from the worm's interior. In contrast, the dead worm's membrane is inactive due to irreversible permeation²². Additionally, to trap a live worm, the electrostatic forces must overcome the worm's muscular force. As a result, dead worms are trapped much more readily than live ones, and DEP can be used to remove dead worms from the suspension.

Our experiments focused on L1, L3, and adult worms. The worms were introduced, one at a time, at the entrance of the conduit and guided by a gentle flow towards the active electrodes (see Supplementary Information for the experimental procedures and worm preparation). When the electric field intensity was sufficiently high, the electric field exerted a force on the worm and confined the worm in the vicinity of the electrode tips. As a measure of the electric field intensity, we use the root-mean-square of the electrical potential (V_{rms}) across the electrode pair divided by the shortest distance between the two electrodes.

Fig. 2a (top) is a photograph of a trapped adult worm. When the distance between the electrodes exceeded the worm's body length, the worm's tail ended up tethered to one of the electrodes, while its more energetic head was positioned away from the electrode and free to move (Supplementary Movie S1). The threshold electric field needed to trap worms is denoted E_{c1} . The two photographs at the bottom of Fig. 2a are superimposed images of the untrapped (left, $E=0$) and trapped (right, $E>E_{c1}$) worms during a swimming cycle. The motions of the trapped and untrapped worms appear to be qualitatively similar. Once the electric field was turned off, the released worms resumed their normal behavior. In summary, when the electric field intensity did not far exceed E_{c1} , the trapped worm's motion was comparable to that of a freely swimming worm (in the absence of an electric field) and the worm appeared to be unharmed.

Fig. 2b depicts the adult worm's body curvature as a function of position along the worm's length (vertical axis) and time (horizontal axis) prior to trapping (top), during trapping (middle), and after release (bottom). To this end, the two-dimensional projection of the worm's body was approximated with a line drawn along the body's center from head to tail. The curvature of the centerline was then calculated as a function of position and time with Matlab²³. The red and blue colors represent, respectively, high (4.5 rad/mm) and low (-4.5 rad/mm) curvatures. The kinematics of the motion before, during, and after trapping, all appear similar. After the experiment, the released worm laid eggs and appeared to behave normally.

The effect of the electric field on the worms' photophobic response was also examined. Worms normally avoid the ultraviolet component of direct sunlight^{24, 25}. Fig. 2c depicts the planar projection of the head trajectories of the DEP-trapped worm when illuminated with blue (480 nm) and green (545 nm) light sources. The illuminated area is circled with a dashed line. The trajectories indicate that the trapped worm is oblivious to the green light but maneuvers to avoid the blue light (Supplementary Movie S2). This apparent photophobic response implies that the light-sensitive neurons remain intact in the presence of the electric field used for the DEP trapping. In addition to the above two viability tests, a DEP trapped worm also showed normal electrosensation in a DC electric field. Although more measurements need to be done to support the assumption, the preliminary test appeared to be in agreement with the observation of harmless DEP.

Fig. 2d depicts the normalized variance (circles) and normalized frequency (squares) of the L2 worm's fluctuations (see Supplementary Data for definitions) as functions of the electric field frequency ($n=3$) at a potential difference across the electrodes of 11 V_{rms} . The data were normalized with the variance and frequency of the worms prior to their trapping. At low electric field frequencies, the worms are sluggish, suggesting possible injury. In contrast, the level of activity of worms subjected to higher frequencies resembles the behavior of worms in the absence of an electric field. The left and right vertical scales are shifted to improve clarity.

Fig. 2e depicts the variance (solid circles) and frequency (solid squares) of L2 worms as functions of electric field intensity ($n=3$) at an electric field frequency of 800 kHz. At low

and moderate electric field intensities, the worm's motion resembles that of freely swimming worms in the absence of an electric field. As the electric field intensity increases above a certain threshold (E_{c2}), the worm's motility decreases or ceases, implying possible injury or death. The critical electric field magnitude needed to induce injury or paralysis increases as the worm's size increases. Whether injury or death results (when $E > E_{c2}$) depends on the length of time that the worms remain exposed to the electric field and on the electric field's magnitude. When the electric field's magnitude is not too high ($E_{c2} < E < E_{c3}$) and the exposure time is relatively short, injured/paralyzed worms seem to regain their vitality once removed from the electric field. Prolonged exposure and/or high electric fields cause death.

Next, we investigated the behaviors of various size worms from larval stage to adulthood as a function of the electric field intensity and frequency. Fig. 3a delineates qualitatively the behavior of *C. elegans* in various domains of the electric field intensity - frequency space. The positions of the boundaries between the various domains depend on the worms' size, but are not sharply defined even within a homogeneous population of same size worms. When the electric field frequency (ω) and intensity (E) are low, the cuticle/membrane isolates the worm's body from the electric field, reducing the worm's polarizability and DEP tendency. When the frequency is very low (< 10 Hz), the worm can overcome the electrokinetic forces and exhibit electrotaxis, which is a behavioral response¹⁷⁻¹⁹. When the frequency is larger than 10 Hz and the field intensity is lower than a threshold value $E_{c0}(\omega)$ or $E_{c1}(\omega)$, the worm appears oblivious to the presence of the electric field. When $E_{c1}(\omega) < E < E_{c2}(\omega)$ and $\omega > 100$ kHz, the worms are trapped without any apparent injury (Supplementary Movie S1). When $E_{c2}(\omega) < E < E_{c3}(\omega)$ and $\omega > 10$ kHz, the worms are trapped and eventually paralyzed by the electric field. The latency to paralysis depends inversely on the electrical field's magnitude. When $E_{c0}(\omega) < E < E_{c3}(\omega)$ and $\omega < 10$ kHz, the worms are paralyzed but not trapped. At lower electric field intensities and relatively short exposure times, the paralysis appears reversible. Once the field is turned off, the worm seems to resume its normal behavior (Supplementary Movie S3). At higher field intensities or higher exposure times, however, the injury appears permanent. At even higher field intensities ($E > E_{c3}$), the worms are killed. The boundaries of the trapping domain are delineated by the curves E_{c4} and E_{c1} , which together form a parabolic shape. Qualitatively, this is the inverse of the behavior of the Clausius-Mossotti factor $K(\omega)$ depicted in Fig. 1d. At relatively low frequencies, the membrane shields the worm's interior from the electric field ($K(\omega)$ is small) and higher electric fields are needed to trap the worm. As the frequency increases, $K(\omega)$ increases, and the magnitude of E_{c4} decreases. Once the frequency is increased above the value at which $K(\omega)$ attains maximum, the magnitude of the electric field needed for trapping increases as the $K(\omega)$ factor decreases.

In contrast to low frequency stimulation, which results in a behavioral response only in larger ($> L2$) worms¹⁷, positive DEP successfully traps worms of all stages and sizes, which further supports the hypothesis that the trapping mechanism reported here is distinct from electrotaxis and low-frequency localization previously reported¹⁷⁻²⁰.

The magnitude of the electric field needed to overcome the worm's muscular force depends on the worm's size. Fig. 3b depicts the effect of the electric field magnitude on worms as a function of the worm's size when the field frequency is 800 kHz. The color gradients are used to emphasize that the boundaries between the various domains are not sharply defined. The first, second, and third bars correspond, respectively, to L1 (length $\sim 223 \pm 39$ μm), L3 ($\sim 480 \pm 43$ μm), and adult ($\sim 1217 \pm 139$ μm) stage worms. The lowest (purple) domain of each bar corresponds to electric field intensities that have no apparent effect on the worms. The second (blue) domain corresponds to the trapping phase; the third (green) domain to the paralyzing domain, and the top (red) to the domain when worms are visibly harmed. We

expected that as the size of the worm increases, the muscular power of the worm would increase but the threshold electric field needed to trap would decrease because DEP force is proportional to the worm's volume. We in fact observed that the DEP force necessary to trap adult worms is slightly lower than that needed to trap L3 worms, suggesting that the worm's volume and muscular power do not increase at the same rate in proportion to size.

Fig. 3c illustrates worm behavior as a function of size and field frequency. Each bar corresponds to a different size worm and different electric field magnitude. The first, second, and third bars correspond, respectively, to L1 ($6 V_{\text{rms}}$), L3 ($16 V_{\text{rms}}$), and adult ($15 V_{\text{rms}}$) worms. Different electric field magnitudes were used as different size worms require different threshold electric fields for trapping. At low and moderate frequencies, the worms are harmed by the field. At high frequencies, the worms appear to tolerate the electric field even when trapped. Figs. 3b and 3c indicate that by varying the magnitude of electrical field at a fixed frequency, one can use positive DEP to sort worms according to size.

Once worms have been trapped, they do not necessarily remain attached to the electrodes indefinitely. Some worms manage to maneuver out of the trap after a certain time interval Δt . To escape, the worms align themselves with the electrode's surface so that the electric field gradients and the DEP force are reduced. Figs. 3d, 3e, and 3f depict the trapping duration τ as a function of the field frequency and intensity of L1, L3, and adult worms, respectively. The larger the electric field intensity, the longer the trapping duration.

Most of our observations were carried out at electric field frequencies much greater than 10 Hz. Hence, the phenomenon described here is likely caused by the electric polarization of the worm's body and not by electrotaxis. In other words, the worms are subjected to positive DEP. Although DEP has been widely used to sort and position nano particles, macromolecules, and cells, this is the first report on the use of DEP to manipulate animals. Surprisingly, there is a region of electric field magnitudes and frequencies which appears to leave the worms unharmed. To trap the worms, the dielectrophoretic force must overcome the worm's muscular force, which increases with worm size. At the same time, DEP force is directly proportional to volume. Because the rate of muscular force increase and the rate of DEP force increase with volume are not necessarily identical, the electrical field intensity needed for trapping varies in a complicated way as a function of the worm's size. For example, an L3 stage worm requires trapping field intensities that are greater than both L1 and adult stage worms trapping intensities. DEP can be used to apply a remotely controlled force to worms. Based on the normal body movements and photo avoidant behavior we observed in trapped worms, it appears that many biological functions are preserved under positive DEP trapping forces. Potential applications include, among other things, sorting of worms by size, removing dead worms from solution, and tethering worms at predetermined positions for biological studies such as hydrodynamic interactions between worms.

Supplementary Material

Refer to Web version on PubMed Central for supplementary material.

Acknowledgments

We are grateful to Dr. Paulo Arratia and Mr. Xiaoning Shen for their advice and technical assistance.

references

1. Morgan H, Green NG. J. Electrostatics. 1997; 42:279–293.
2. Fiedler S, Shirley SG, Schnelle T, Fuhr G. Anal. Chem. 1998; 70:1909–1915. [PubMed: 9599586]

3. Ying L, White SS, Bruckbauer A, Meadows L, Korchev YE, Klenerman D. *Biophys. J.* 2004; 86
4. Brenner S. *Br. Med. Bull.* 1973; 29:269–271. [PubMed: 4807330]
5. Brenner S. *Genetics.* 1974; 77:71–94. [PubMed: 4366476]
6. Bargmann CI. *Ann. Rev. Neurosci.* 1993; 16:47–71. [PubMed: 8460900]
7. Whittaker AJ, Sternberg PW. *Curr. Opin. Neurobiol.* 2004; 14:450–456. [PubMed: 15321066]
8. Hobert O. *J. Neurobiol.* 2002; 54:1–3. [PubMed: 12486696]
9. Kwok TCY, Ricker N, Fraser R, Chan AW, Burns A, Stanley EF, McCourt P, Cutler SR, Roy PJ. *Nature.* 2006; 441:91–95. [PubMed: 16672971]
10. Hulme SE, Shevkopyas SS, Apfeld J, Fontana W, Whitesides GM. *Lab. Chip.* 2007; 7:1515–1523. [PubMed: 17960280]
11. Guo SX, Bourgeois F, Chokshi T, Durr NJ, Hilliard MA, Chronis N, Ben-Yakar A. *Nat. Methods.* 2008; 5:531–533. [PubMed: 18408725]
12. Chung K, Crane M, Lu H. *Nat. Methods.* 2008; 5:637–643. [PubMed: 18568029]
13. Crowder CM, Shebestor LD, Schedl T. *Anesthesiology.* 1996; 85:901–912. [PubMed: 8873562]
14. Kerr R, Lev-Ram V, Baird G, Vincent P, Tsien RY, Schafer WR. *Neuron.* 2000; 26:583–594. [PubMed: 10896155]
15. Faumont S, Lockery SR. *J. Neurophysiol.* 2005; 95:1976–1981. [PubMed: 16319197]
16. Chronis N, Zimmer M, Bargmann CI. *Nat. Methods.* 2007; 4:727–731. [PubMed: 17704783]
17. Rezaei P, Siddiqui A, Selvaganapathy PR, Gupta BP. *Appl. Phys. Lett.* 2010; 96:153702.
18. Rezaei P, Siddiqui A, Selvaganapathy PR, Gupta BP. *Lab. Chip.* 2010; 10:220–226. [PubMed: 20066250]
19. Gabel CV, Gabel H, Pavlichin D, Kao A, Clark DA, Samuel ADT. *J. Neurosci.* 2007; 27:7586–7596. [PubMed: 17626220]
20. Sukul NC, Croll NA. *J. Nematol.* 1978; 10:314–317. [PubMed: 19305860]
21. Morgan, H.; Green, NG. *AC Electrokinetics: colloids and nanoparticles.* Research Studies Press Ltd; Baldock, Hertfordshire, England: 2002.
22. Jen CP, Chen TW. *Biomed. Microdevices.* 2009; 11:597–607. [PubMed: 19104941]
23. Sznitman J, Purohit PK, Krajacic P, Lamitina T, Arratia PE. *Biophys. J.* 2010; 98:617–626. [PubMed: 20159158]
24. Ward A, Liu J, Feng Z, Xu XZS. *Nat. Neurosci.* 2008; 11:916–922. [PubMed: 18604203]
25. Edwards SL, Charlie NK, Milfort MC, Brown BS, Gravlin CN, Knecht JE, Miller KG. *PLoS Biol.* 2008; 6:1715–1729.

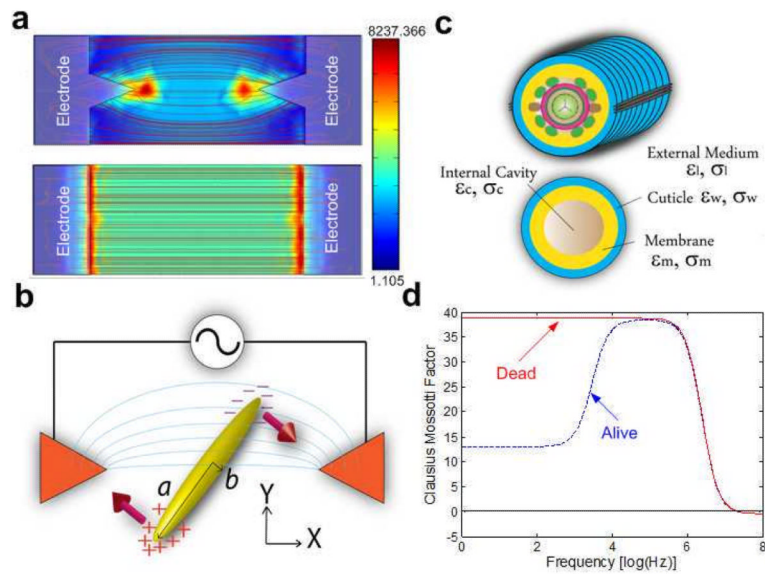


Fig. 1.

(a) Two different electrode patterns used in the experiments: spiked electrodes (top) and flat electrodes (bottom). The red lines correspond to a top view of the computed electric field lines (Finite Element simulation of the electric field with Comsol Multiphysics). The intensity of the electric field is indicated by color ranging from blue (least intense) to red (most intense). (b) Conceptual depiction of the electrical polarization forces acting on a prolate spheroid positioned between the spiked electrodes. (c) A crude model of *C. elegans* as a shell containing organs (top) and a homogeneous core (bottom). (d) The estimated Clausius-Mossotti factor $K(\omega)$ (Eq. 1) of a live and a dead *C. elegans* as functions of field frequency (see Supplementary Data).

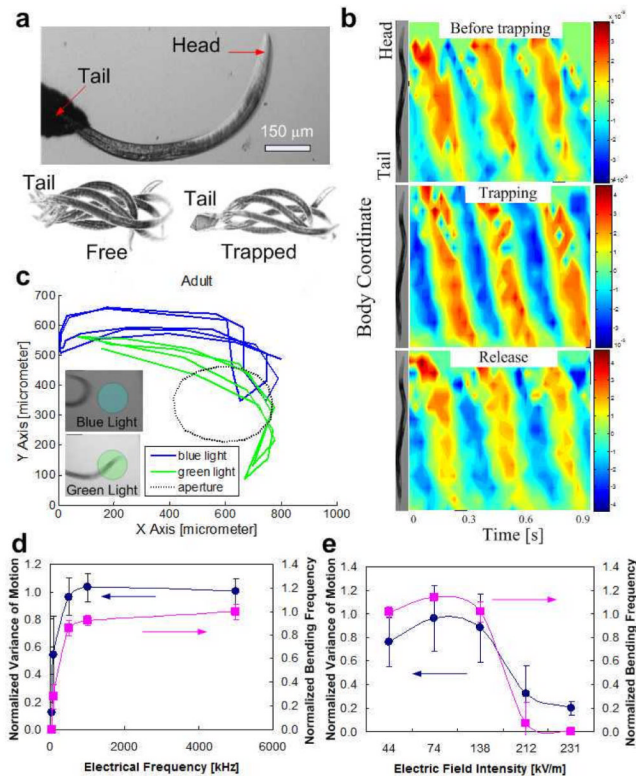


Fig. 2.

(a) (Top): Photograph of an adult worm trapped in the electric field. The applied potential difference between the electrodes is $30 V_{\text{rms}}$ (500 kHz). (Bottom): Superimposed images of free (left) and trapped (right) worms during one swimming cycle. (b) The worm's body curvature as a function of position along the worm's body coordinate and time before (top), during (middle), and after (bottom) release. The color represents the magnitude of the bending angle from extreme ventral bend (red) to extreme dorsal bend (blue). (c) Head trajectories of DEP trapped worm when illuminated with blue (blue line) and green (green line) light sources. The dashed circle indicates the illuminated area. The worm avoids diligently the blue light (inset, top) while it does not mind the green light (inset, bottom). (d-e) The normalized variance (solid circles) and normalized frequency (solid squares) of L2 worm's fluctuations as functions of electric field frequency when the potential difference across the electrodes is $11 V_{\text{rms}}$ (d) and electric field intensity when the electric field frequency is 800 kHz (e).

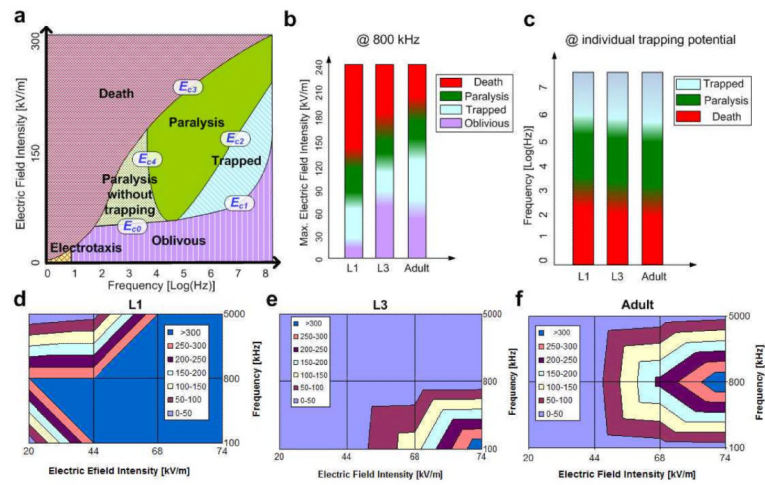


Fig. 3. (a) The behavior of *C. elegans* as a function of field intensity and frequency. (b) The behavior of L1, L3, and adult worms as functions of electric field intensity when the frequency is 800 kHz. (c) The behavior of L1 (6 Vrms), L3 (16 Vrms), and adult (15 Vrms) worms as functions of the frequency. (d-f) Trapping duration Δt (s) of L1 (d), L3 (e), and adult (f) stage worms as a function of electric field frequency and intensity.